

Phase separation and collapse in Bose-Fermi mixtures with a Feshbach resonance

F. M. Marchetti,^{1,*} C. Mathy,² M. M. Parish,^{2,3,†} and D. A. Huse²

¹*Rudolf Peirels Centre for Theoretical Physics, University of Oxford, 1 Keble Road, Oxford OX1 3NP, UK*

²*Department of Physics, Princeton University, Princeton, New Jersey 08544, USA*

³*Princeton Center for Theoretical Physics, Princeton University, Princeton, New Jersey 08544, USA*

(Dated: February 21, 2019)

We consider a mixture of single-component bosonic and fermionic atoms with an interspecies interaction that is varied using a Feshbach resonance. By performing a mean-field analysis of a two-channel model, which describes both narrow and broad Feshbach resonances, we find an unexpectedly rich phase diagram at zero temperature: Bose-condensed and non-Bose-condensed phases form a variety of phase-separated states that are accompanied by both critical and tricritical points. We discuss the implications of our results for the experimentally observed collapse of Bose-Fermi mixtures on the attractive side of the Feshbach resonance, and we make predictions for future experiments on Bose-Fermi mixtures close to a Feshbach resonance.

The possibility of controlling the inter-atomic interaction strength via Feshbach resonances has recently played a pivotal role in investigating new condensation phenomena in ultracold alkali gases. A prominent example is the realization of condensed pairs in two-component Fermi gases, where one has a crossover from the weakly-interacting BCS regime to a Bose-Einstein condensate (BEC) of diatomic molecules [1]. By tuning the two spin populations to be unequal, one can further explore quantum phase transitions and phase separation (see, e.g., [2] and references therein). Even richer scenarios are expected for heteronuclear resonances in Bose-Fermi mixtures, because one can in principle destroy the BEC by binding bosons and fermions into *fermionic* molecules [3]. Moreover, a host of novel phases has been predicted, such as spatial separation of bosons and fermions induced by interspecies repulsive interactions [4, 5], boson-mediated Cooper pairing [6], density wave phases in optical lattices [7], and the formation of polar molecules with dipolar interactions.

Following the recent detection of Feshbach resonances in Bose-Fermi mixtures [8, 9], experiments have begun to explore how the behavior of the ⁴⁰K-⁸⁷Rb system depends on the interspecies interaction strength [10, 11, 12]. Thus far, repulsive interactions (generated by approaching the resonance from the side of positive scattering length a_{BF}) have been observed to reduce the spatial overlap between fermions and the BEC. By contrast, attractive interactions can produce a sudden loss of atoms, which has been attributed to enhanced three-body recombination processes resulting from an unconstrained increase in the density. Current mean-field theories [4, 13, 14] predict that this *total* collapse of the mixture occurs above a critical density or interaction strength, where the mixture is dynamically unstable. However, these theories neglect any pairing between bosons and fermions, which we show plays a crucial role in the stability of the system.

In this Letter, we address the possibility of pairing in Bose-Fermi mixtures by considering a two-channel model

that explicitly includes fermionic molecules as an extra species of particle. Such a model encompasses both broad and narrow Feshbach resonances. We then determine the zero-temperature phase diagram for the Bose-Fermi mixture as a function of the interaction strengths and particle densities within a mean-field approximation. Sufficiently close to the resonance, we always find phase separation between a mixed BEC phase (where the BEC coexists with fermions) and either a pure BEC, mixed BEC, normal or vacuum phase (see Fig. 1). To our knowledge, this provides the first example of phase separation in a Bose-Fermi mixture with *attractive* interactions — e.g., ³He-⁴He mixtures [15] and polarized Fermi gases [2] require effectively repulsive interactions. We explain why our results are consistent with the collapse observed in current experiments and we discuss the best conditions for observing the predicted phase separation.

As in Ref. [3], the two-channel Hamiltonian,

$$\hat{H} = \sum_{\mathbf{k}} \left(\xi_{\mathbf{k}}^f f_{\mathbf{k}}^\dagger f_{\mathbf{k}} + \xi_{\mathbf{k}}^b b_{\mathbf{k}}^\dagger b_{\mathbf{k}} + \xi_{\mathbf{k}}^\psi \psi_{\mathbf{k}}^\dagger \psi_{\mathbf{k}} \right) + \frac{g}{\sqrt{V}} \sum_{\mathbf{k}, \mathbf{k}'} \times \left(\psi_{\mathbf{k}+\mathbf{k}'}^\dagger f_{\mathbf{k}} b_{\mathbf{k}'} + \text{h.c.} \right) + \frac{\lambda}{V} \sum_{\mathbf{k}, \mathbf{k}', \mathbf{q}} b_{\mathbf{k}}^\dagger b_{\mathbf{k}'}^\dagger b_{\mathbf{k}'+\mathbf{q}} b_{\mathbf{k}-\mathbf{q}}, \quad (1)$$

describes a mixture of bosonic b and fermionic f atoms coupled to a *fermionic* closed channel molecule ψ , where V is the three-dimensional volume. Setting $\hbar = 1$, $\xi_{\mathbf{k}}^f = \mathbf{k}^2/2m_f - \mu_f$, $\xi_{\mathbf{k}}^b = \mathbf{k}^2/2m_b - \mu_b$ and $\xi_{\mathbf{k}}^\psi = \mathbf{k}^2/2(m_b + m_f) - \mu_f - \mu_b + \nu$, where ν is the detuning. The two-channel model (1) describes both narrow ($\gamma^2/k_B(T_0 + T_F) \ll 1$) and wide ($\gamma^2/k_B(T_0 + T_F) \gg 1$) Feshbach resonances, where the width of the resonance

$$\gamma = \frac{g^2}{8\pi} m^{3/2}, \text{ with } m = \frac{2m_f m_b}{m_f + m_b}, \quad (2)$$

is compared to the boson condensation temperature ($k_B T_0 = 2\pi[n_b/g_{3/2}(1)]^{2/3}/m_b$ with $g_{3/2}(1) \simeq 2.612$) and the Fermi energy ($k_B T_F = (6\pi^2 n_f)^{2/3}/2m_f$). In the following we fix $m_f/m_b \simeq 0.46$ as in ⁴⁰K-⁸⁷Rb mixtures, although different mass ratios will not change

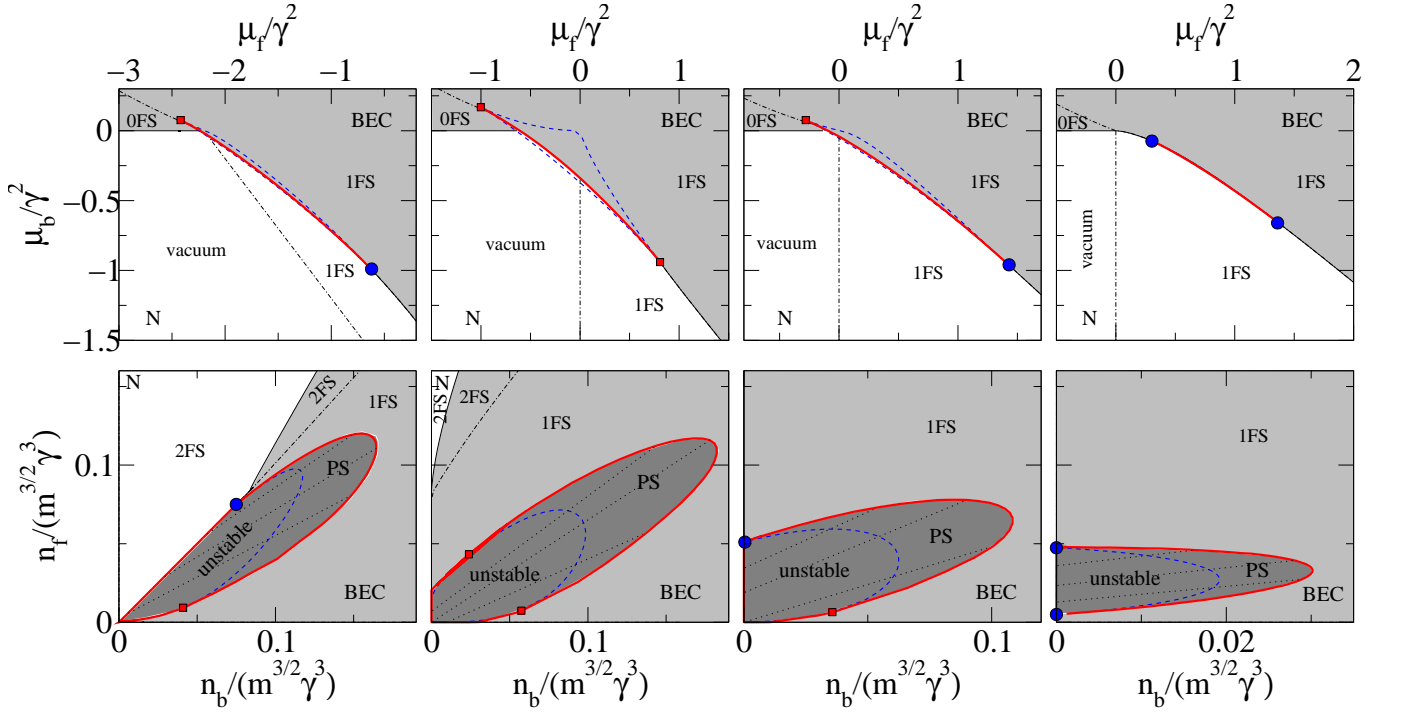


FIG. 1: (Color online) Zero temperature, mean-field phase diagrams for fixed $\lambda m_b^{3/2} \gamma \simeq 4.66$, where the top and bottom rows correspond to chemical potential and density space, respectively, while the columns represent different detunings: $\nu/\gamma^2 = -2.2$ (first), $\nu/\gamma^2 = 0$ (second), $\nu/\gamma^2 = 1$ (third) and $\nu/\gamma^2 = 1.75$ (fourth). The various phases can be distinguished based on the number of Fermi surfaces (FS) and whether or not there is a BEC (light gray shaded region). The solid thick (red) lines represent first-order phase transitions, which are accompanied by regions of phase separation (PS — dark gray shaded region) in density space, while the thin solid (black) lines of the phase boundaries are continuous. The dotted lines that connect points on the first-order boundary depict which phases constitute the phase-separated state at a given density. A filled (blue) circle denotes a tricritical point, a filled (red) square denotes a critical point, and a dashed (blue) line denotes a spinodal line.

our results qualitatively. At zero temperature, Eq. (1) can be exactly diagonalized in the mean-field approximation, $\langle b_{\mathbf{k}} \rangle = \delta_{\mathbf{k},0} \sqrt{V} \Phi$, implying that the two Fermi species dispersions, ξ^f and ξ^ψ , are now hybridized by the presence of the condensate, $\xi^{F,\Psi} = (\xi^f + \xi^\psi)/2 \pm \sqrt{(\xi^f - \xi^\psi)^2 + 4g^2 \Phi^2}/2$. This leads to the following expression for the grand-canonical free energy density $\Omega^{(0)}(\mu_f, \mu_b) = \min_{\Phi} f(\Phi; \mu_f, \mu_b)$:

$$f(\Phi; \mu_f, \mu_b) = \frac{1}{V} \sum_{\mathbf{k}} [\Theta(-\xi_{\mathbf{k}}^F) \xi_{\mathbf{k}}^F + \Theta(-\xi_{\mathbf{k}}^\Psi) \xi_{\mathbf{k}}^\Psi] - \mu_b \Phi^2 + \lambda \Phi^4. \quad (3)$$

As experiments are performed at fixed densities, the chemical potentials μ_f and μ_b have to be determined from the total number of fermionic and bosonic atom densities, $n_{f,b} = -\partial \Omega^{(0)}/\partial \mu_{f,b}$ [25]. Note that our mean-field analysis is only quantitatively accurate in the case of narrow Feshbach resonances, because Gaussian fluctuations beyond mean-field scale like $\gamma/\sqrt{k_B(T_0 + T_F)}$ [16]. However, we expect it to provide a qualitative description of pairing in systems with a broad Feshbach resonance, as is the case in two-component Fermi gases [26]. In-

deed, pairing instabilities have been shown to exist in single-channel models that approximate broad Feshbach resonances [17].

If one focusses on pairing only, it is clear that at the fixed density $n_f \geq n_b$ there is a transition as we cross the resonance: the BEC phase ($\Phi \neq 0$) will be completely depleted ($\Phi = 0$) by the binding of bosons into fermionic molecules [27]. This transition was shown to be continuous for the limiting case of vanishing coupling $g = 0$ [18]. Assuming the transition remains second order for $g \neq 0$, as in Ref. [3], the boundaries are found by solving $O(\Phi^2) \equiv \partial f/\partial \Phi^2|_{\Phi=0} = 0$. However, in general we find that there can also be first order transitions between two BEC phases as well as between BEC and normal (N) phases, even when $n_f < n_b$. Before we explain the main features of the phase diagram (Fig. 1), it is useful to examine how the second order transition becomes first order.

Precursors of first order transitions can be found in tricritical points, where $O(\Phi^4) \equiv \partial^2 f/\partial (\Phi^2)^2|_{\Phi=0} = 0$. Surprisingly, the mean-field energy $f(\Phi; \mu_f, \mu_b)$ can be expressed in terms of just three independent dimensionless parameters, and thus the phase transi-

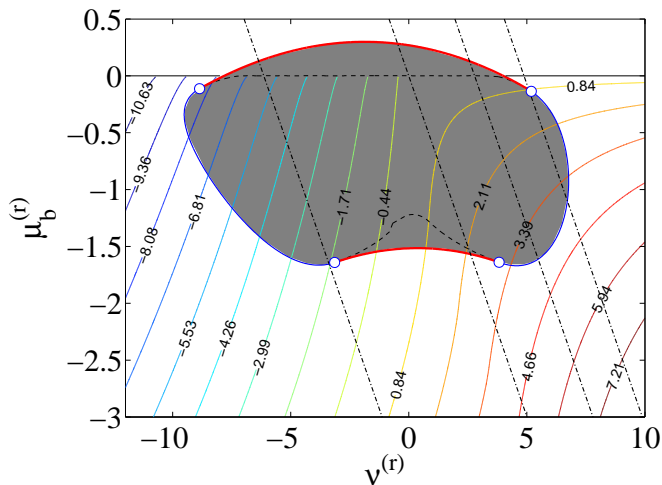


FIG. 2: (Color online). Boundary of the surface of first-order phase transitions in the 3D space $\{\mu_f^{(r)}, \nu^{(r)}, \mu_b^{(r)}\} \equiv c^{1/3}\{c^{1/3}\mu_f/\gamma^2, c^{1/3}(\nu - \mu_b)/\gamma^2, \mu_b/\gamma^2\}$, where $c = \lambda m_b^{2/3}\gamma$, that has been projected onto the $(\nu^{(r)}, \mu_b^{(r)})$ plane. The thick lines enclose the first-order region (gray shaded region), while the contour lines at constant $\mu_f^{(r)}$ represent the surface of second-order BEC-N phase transitions, where the BEC phase lies above the surface. For $|\nu^{(r)}|$ greater than the tetracritical points $O(\Phi^2) = O(\Phi^4) = O(\Phi^6) = 0$ (open circles), the (blue) thick line consists of tricritical points that lie on the second-order surface. Otherwise, they are replaced by critical endpoints (dashed line), where first and second order transition lines intersect, and critical points [thick (red) line]. The dotted-dashed straight lines correspond to the cuts at fixed ν/γ^2 and c in Fig. 1, where we have $c \simeq 4.66$ and $\nu/\gamma^2 = -2.2, 0, 1, \text{ and } 1.75$, going from left to right.

tions can be completely characterized by the parameters $\{\mu_f^{(r)}, \nu^{(r)}, \mu_b^{(r)}\}$ introduced in Fig. 2. The ratio λ/γ^2 sets the scale of $\{\mu_f^{(r)}, \nu^{(r)}\}$ and determines when the tricritical points are replaced by critical points and critical endpoints: Here, an expansion in Φ^2 cannot be exploited any longer. Note that this is not so surprising because, when $\lambda = 0$, the mean-field potential (3) is unbounded from below ($f(\Phi \gg 1; \mu_f, \mu_b) \propto -\Phi^{5/2}$). This non-analytic behavior comes from the hybridized Fermi dispersions $\xi^{F,\Psi}$. Note also that one can access the regime of first order transitions even when the repulsion between bosons λ is large, by making μ_f, ν and μ_b sufficiently small — as a consequence we expect these results to apply in the low density limit close to resonance.

While one can parameterize the entire phase diagram using $\{\nu^{(r)}, \mu_b^{(r)}, \mu_f^{(r)}\}$, from the point of view of real systems, it makes more sense to consider the parameters $\{c \equiv \lambda m_b^{3/2}\gamma, \nu/\gamma^2, \mu_b/\gamma^2, \mu_f/\gamma^2\}$. For a given experiment, c is fixed by the typical boson-boson interaction strength and width of the resonance, while ν/γ^2 is determined by the Bose-Fermi scattering length $a_{BF} = -2\gamma/\sqrt{m\nu}$. Therefore, the phase diagram can be

plotted as a function of the chemical potentials (top row of Fig. 1). These slices correspond to planes in Fig. 2 given by $\mu_b^{(r)} = -\nu^{(r)}/c^{1/3} + c^{1/3}\nu/\gamma^2$. To be relevant to current experiments on ^{40}K - ^{87}Rb mixtures, we take $c \simeq 4.66$ and $a_{BF} = -339.3a_0\gamma^2/\nu$, where a_0 is the Bohr radius. However, the qualitative behavior of the phase diagram in Fig. 1 will apply for $c \lesssim 10$. In this limit, first order transitions appear only in the finite interval around unitarity, $c^{2/3}\nu/\gamma^2 \in [-10, 6]$. At the resonance we find two critical points (and two accompanying critical endpoints), while moving far from the resonance in either direction, first one and then both critical points are replaced by tricritical points. In terms of the phase diagram in density space (bottom row of Fig. 1), first order transitions imply phase separation (PS) between BEC and N (BEC and BEC) close to a tricritical (critical) point. Here, N satisfies $n_f = n_b$ when $\nu < 0$ and $n_b = 0$ when $\nu > 0$. Both BEC and N phases can be further characterized by the number of Fermi surfaces (FS). In the N region, the second-order boundaries between regions with different numbers of FS are defined by $\mu_f = 0$ ($n_b = n_f$) and $\mu_b = -\mu_f + \nu$ ($n_b = 0$). In the BEC phase instead one has to impose the condition $g^2\Phi^2 = \mu_f(\mu_f + \mu_b - \nu)$. A special case of PS occurs when the N phase is the vacuum: Physically this is equivalent to a *partial* collapse of the system to higher densities.

Within the PS region it is possible to distinguish a metastable and an unstable (or spinodal) region separated by a spinodal line, where minimum and maximum of $f(\Phi; \mu_f, \mu_b)$ merge. Inside the spinodal region, the dynamics of phase separation following a sudden quench proceeds via a linear instability (see, e.g., [19] and references therein), while it is characterized by nucleation in the metastable region. A calculation of the spinodal lines has also been carried out in Ref. [3] at a fixed n_b , although the possibility of phase separation was not considered. In addition, Ref. [3] suggests that, when $n_f < n_b$, there is a smooth crossover at fixed density from the atomic to the molecular side of the resonance within the same BEC-1FS phase. We find that this crossover exists for sufficiently large densities, while phase separation intervenes at small densities $n_f \lesssim 0.15m^{3/2}\gamma^3$ and $n_b \lesssim 0.2m^{3/2}\gamma^3$ (Fig. 1). More generally, the size of the phase-separated region scales like γ^2/λ for both n_f and the molecular component of n_b , while the condensed component of n_b scales like $\gamma^2/(\lambda c^{1/3})$.

Finally, we note that the narrow Feshbach resonance regime, $\gamma^2/k_B(T_0 + T_F) < 1$, corresponds to densities $n_f > 0.03m^{3/2}\gamma^3$ or $n_b > 0.3m^{3/2}\gamma^3$, therefore our mean-field treatment should be reasonable for much of the region of interest. Certainly, the unstable region is a robust feature of the overall phase diagram, because we can arbitrarily increase the size of it in density-space by decreasing λ/γ^2 or $\lambda c^{1/3}/\gamma^2$.

It is instructive to compare our results for the phase diagram with existing single-channel theories and experi-

ments on Bose-Fermi mixtures. When the effective Bose-Fermi interaction is attractive, $U_{BF} < 0$, the single-channel mean-field theory is formally equivalent to our model (3) in the limit $\nu \rightarrow +\infty$, $g \rightarrow +\infty$, holding $U_{BF} = -g^2/\nu$ fixed. Therefore, pairing correlations $\langle \psi \rangle \sim \langle fb \rangle$ are no longer included, and one can easily show that the single-channel free energy is not bounded from below ($f_{1c}(\Phi \gg 1; \mu_f, \mu_b) \propto -\Phi^5$). As a consequence, any state at finite density is metastable and, above a critical density or interaction strength, the system is unstable to a total collapse [14]. By contrast, in our model, the formation of fermionic pairs stabilizes the large Φ behavior and constrains unbounded increases of densities, leading to phase separation. Close to unitarity, phase separation takes the form of a partial collapse. In current experiments, the typical starting densities are $n_b/m^{3/2}\gamma^3 \sim 2n_f/m^{3/2}\gamma^3 \sim 10^{-4}$, so the phase-separated state in Fig. 1 will involve such a large increase in density that it will be destroyed by three-body recombination, as experimentally observed in the case of attractive interactions [10, 11]. The dominant three-body process involves 1 fermionic atom and 2 bosonic atoms, with recombination rate $\Gamma \propto a_{BF}^4 n_f n_b^2$ away from resonance [20]. Thus, to minimize Γ in the phase-separated state, we must reduce the densities and/or $|a_{BF}|$ at which phase separation first appears. Assuming the bosons are mostly condensed and using the scalings described previously, we get $\Gamma/n_b \propto m^{3/2}\lambda^{1/3}\gamma^{7/8}$ and $\Gamma/n_f \propto m\gamma^2$. Therefore, we must consider small γ , such as the Feshbach resonance for ^{23}Na - ^6Li mixtures [8], and perhaps small λ , although the dependence of Γ on λ is sensitive to the precise power of $|a_{BF}|$, which in turn can depend on the width of the resonance [21].

On the repulsive side of the resonance, $U_{BF} > 0$, the mean-field single channel theory predicts phase separation between atomic bosons and fermions induced by the repulsion [5]. One can instead access the regime of model (1) by starting from $a_{BF} < 0$ and sweeping through the resonance to the molecular side, $a_{BF} > 0$. While most of the experiments have focussed on the repulsive Bose-Fermi interaction, fermionic molecules have been very recently produced [12, 22, 23].

In principle, one can detect phase separation using *in situ* absorption measurements. To extract the behavior of the trapped gas from the uniform phase diagram (Fig. 1), we use the local density approximation to convert the effects of the trap into spatially varying chemical potentials. The spatial trajectory in a trap is then represented by the straight line $\mu_{f,b}(\mathbf{r})/\gamma^2 = \mu_{f,b}(0)/\gamma^2 - V(\mathbf{r})/\gamma^2$ in the phase diagram, assuming that the fermionic and bosonic atoms experience the same harmonic trapping potential $V(\mathbf{r})$ [11]. Phase separation in a trap occurs when the first-order boundary between BEC and N is crossed, yielding a discontinuity in the density profiles. In this case, the central phase is always a BEC (with 1FS), while the surrounding phases can be either

BEC or N (with different numbers of FS). In particular, the partially-collapsed gas will exhibit a sharp interface with the vacuum. The presence of density discontinuities will provide the primary signature for the phase separation predicted here.

We are grateful to J. Chalker, V. Gurarie, P. B. Littlewood, and G. Modugno for stimulating discussions. FMM would like to acknowledge the financial support of EPSRC. This research was supported in part by the National Science Foundation under Grant Numbers PHY05-51164, DMR-0645461 and DMR-0213706.

* Electronic address: fmm25@cam.ac.uk

† Electronic address: mparish@princeton.edu

- [1] C. A. Regal, M. Greiner, and D. S. Jin, Phys. Rev. Lett. **92**, 040403 (2004); M. W. Zwierlein, et al., Phys. Rev. Lett. **92**, 120403 (2004).
- [2] Y. Shin, et al., Phys. Rev. Lett. **97**, 030401 (2006); G. B. Partridge, et al., Phys. Rev. Lett. **97**, 190407 (2006).
- [3] S. Powell, S. Sachdev, and H. P. Büchler, Phys. Rev. B **72**, 024534 (2005).
- [4] K. Mølmer, Phys. Rev. Lett. **80**, 1804 (1998).
- [5] L. Viverit, C. J. Pethick, and H. Smith, Phys. Rev. A **61**, 053605 (2000).
- [6] H. Heiselberg, C. J. Pethick, H. Smith, and L. Viverit, Phys. Rev. Lett. **85**, 2418 (2000).
- [7] M. Lewenstein, L. Santos, M. A. Baranov, and H. Fehrmann, Phys. Rev. Lett. **92**, 050401 (2004).
- [8] C. A. Stan, et al., Phys. Rev. Lett. **93**, 143001 (2004).
- [9] S. Inouye, et al., Phys. Rev. Lett. **93**, 183201 (2004); F. Ferlaino, et al., Phys. Rev. A **73**, 040702 (2006).
- [10] C. Ospelkaus, S. Ospelkaus, K. Sengstock, and K. Bongs, Phys. Rev. Lett. **96**, 020401 (2006); S. Ospelkaus, et al., Phys. Rev. Lett. **97**, 120403 (2006).
- [11] M. Zaccanti, et al., Phys. Rev. A **74**, 041605 (2006).
- [12] G. Modugno (2007), cond-mat/0702277.
- [13] M. Modugno, et al., Phys. Rev. A **68**, 043626 (2003).
- [14] S. T. Chui, V. N. Ryzhov, and E. E. Tareyeva, JETP Lett. **80**, 274 (2004).
- [15] E. H. Graf, D. M. Lee, and J. D. Reppy, Phys. Rev. Lett. **19**, 417 (1967).
- [16] A. V. Andreev, V. Gurarie, and L. Radzihovsky, Phys. Rev. Lett. **93**, 130402 (2004).
- [17] M. Y. Kagan, I. V. Brodsky, D. V. Efremov, and A. V. Klaptsov, Phys. Rev. A **70**, 023607 (2004); A. Storozhenko, et al., Phys. Rev. A **71**, 063617 (2005).
- [18] H. Yabu, Y. Takayama, and T. Suzuki, Physica B **329-333**, 25 (2003).
- [19] A. Lamacraft and F. M. Marchetti, cond-mat/0701692.
- [20] J. P. D’Incao and B. D. Esry, Phys. Rev. Lett. **94**, 213201 (2005).
- [21] D. S. Petrov, Phys. Rev. Lett. **93**, 143201 (2004).
- [22] C. Ospelkaus, et al., Phys. Rev. Lett. **97**, 120402 (2006).
- [23] J. J. Zirbel, et al., arXiv:0710.2479v1 [cond-mat.other].
- [24] M. M. Parish, F. M. Marchetti, A. Lamacraft, and B. D. Simons, Nature Phys. **3**, 124 (2007).
- [25] Note that n_f (n_b) includes fermions (bosons) bound into molecules.
- [26] The phase diagram for polarized Fermi gases is qual-

itatively similar for broad and narrow Feshbach resonances [24].

[27] The formation of molecules can also involve a phase tran-

sition where the number of Fermi surfaces changes.